

IMPACT RESPONSE OF A FINITE CRACK IN PLANE EXTENSION†

G. C. SIH and G. T. EMBLEY

Department of Mechanical Engineering and Mechanics, Lehigh University, Bethlehem, Pennsylvania 18015

and

R. S. RAVERA

Bellcomm Incorporated, Washington D.C. 20024

Abstract—The transient stress and displacement fields around a finite crack opened out by normal and shear tractions applied to its surface are obtained using integral transforms coupled with the technique of Cagniard. The tractions are applied suddenly to the crack which simulates the case of impact loading. By subtracting a uniform state of stress, the present solution also applies to the problem of the sudden appearance of a crack in a pre-stressed body. The results show that significant differences exist between the dynamic stress-intensity factors obtained in this problem and those resulting from static loading. In particular, the energy released by the dynamically loaded crack which is associated with the stress-intensity factor varies with time reaching a maximum very quickly and then oscillates about the static value. The information gained is useful in determining the condition of crack propagation under impact.

INTRODUCTION

OF CONSIDERABLE importance in structural analysis is the transient response of a flaw to a time dependent stress field. The solutions to problems of this type could be applied equally well to cracks in an aircraft wing or to faults in the lithosphere of the earth for example.

A number of papers on the area of dynamic crack analysis have been reviewed in [1]. Recently, the response of a penny shaped crack to various types of transient loads has been considered in papers by Embley and Sih [2] and Sih and Embley [3]. Some other works that specifically deal with transient responses of flaws with finite dimensions have been discussed in Refs. [2, 3] and are due to Flitman [4], Kostrov [5], Eshelby [6] and Achenbach [7, 8]. With the exception of Flitman who considered the far-field solutions to the problem of the sudden appearance of a crack in an elastic media, the authors mentioned have used mathematical techniques successful so far for the case of anti-plane shear only.

The sudden appearance of a semi-infinite crack in an elastic media has been considered by Kostrov [5] for the case of anti-plane loading and by Maue [9] and Baker [10] for the problem of normal tractions. Although these solutions become unbounded as $t \rightarrow \infty$

† This paper is the result of research sponsored by the U.S. Air Force, Eglin Air Force Base under Contract F08635-70-C-0120.

the near field solutions are valid near one tip of a finite crack for the initial period of time before interaction with the stress waves emanating from the other crack tip occurs.

In this paper, the complete near field solution to the problem of a finite line crack subjected to transient in-plane loading will be considered. In conjunction with this, it should be noted that experimental results have been reported by Soltesz and Sommer [11] which have a direct bearing on the theoretical results presented here. The aforementioned authors experimentally determined the time-dependent dynamic stress-intensity factor due to normal loading of a crack by measuring crack opening displacement. The measurements were made on a glass plate by using an optical interference technique and high speed photography. A shock wave formed in a conventional shock tube was used to cause a step function pressure increase on the end face of the cracked plate. Although wave reflection at the boundaries of the finite plate makes interpretation difficult, the order of magnitude of the response compares favorably with the results obtained in this paper.

The specific geometry to be considered here is an infinite elastic plate containing a through-the-thickness line crack oriented as shown in Fig. 1. The transient response

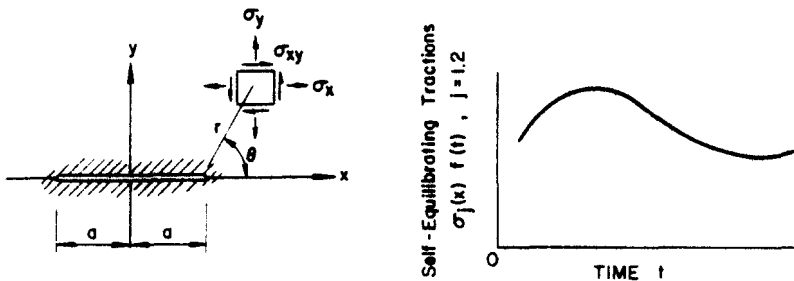


FIG. 1. Crack geometry and stress components.

of the material in the neighborhood of the crack tip will be obtained for two cases. The first deals with the sudden application of self-equilibrating normal tractions to the crack surface. For mathematical simplicity the load is separable into a spatial and temporal function where the spatial function is even in x . Symmetry conditions then enable the problem to be solved in the upper half-space only [12]. The results are directly applicable to the sudden fracture of a plate due to impact caused by projectile penetration. This is modeled as the case of a crack appearing suddenly in a pre-stretched plate which is mathematically equivalent to the problem of applying sudden tractions to the crack surface.

The second case pertains to sudden in-plane shear tractions applied to the crack surface. If the tractions on the upper and lower crack surfaces are equal in magnitude and opposite in sign then symmetry conditions again allow solution in the upper half-plane only. Additional simplicity is obtained by requiring that the spatial component of the load be even in x .

In both cases the method of solution will be to reduce the mixed boundary value problem to a standard Fredholm integral equation in the Laplace transform variable and subsequently invert the Laplace transforms of the stress components by a combination of numerical means and an application of the Cagniard inversion technique. This method was used for the transient problem of anti-plane strain by Ravera and Sih [13].

FORMULATION OF PROBLEM

For plane elastodynamic problems, the displacement component may be expressed in terms of two scalar potentials $\phi(x, y, t)$ and $\psi(x, y, t)$, so that

$$\begin{aligned} u &= -\frac{\partial\phi}{\partial x} + \frac{\partial\psi}{\partial y} \\ v &= -\frac{\partial\phi}{\partial y} - \frac{\partial\psi}{\partial x} \end{aligned} \quad (1)$$

where ϕ and ψ satisfy the second order partial differential equations

$$\nabla^2\phi = \frac{1}{c_1^2} \frac{\partial^2\phi}{\partial t^2}, \quad \nabla^2\psi = \frac{1}{c_2^2} \frac{\partial^2\psi}{\partial t^2} \quad (2)$$

with ∇^2 being the Laplacian operator. The dilatational and shear wave velocities are, respectively

$$c_1 = [(\lambda + 2\mu)/\rho]^{\frac{1}{2}}, \quad c_2 = (\mu/\rho)^{\frac{1}{2}}$$

with λ and μ being the Lamé constants.

Applying the strain-displacement and constitutive equations for a homogeneous isotropic elastic media the stresses may be written in terms of ϕ and ψ as,

$$\begin{aligned} \sigma_x &= -\rho c_1^2 \nabla^2\phi + 2\rho c_2^2 \frac{\partial}{\partial y} \left(\frac{\partial\psi}{\partial x} + \frac{\partial\phi}{\partial y} \right) \\ \sigma_y &= -\rho c_1^2 \nabla^2\phi - 2\rho c_2^2 \frac{\partial}{\partial x} \left(\frac{\partial\psi}{\partial y} - \frac{\partial\phi}{\partial x} \right) \\ \tau_{xy} &= -\rho c_2^2 \left(\frac{\partial^2\psi}{\partial x^2} - \frac{\partial^2\psi}{\partial y^2} + 2 \frac{\partial^2\phi}{\partial x\partial y} \right). \end{aligned} \quad (3)$$

Problem A—symmetric in-plane extension

For zero initial conditions, the stress and displacement field due to sudden application of normal tractions to the crack surface may be found by solving the preceding field equations subject to zero initial conditions, and the following boundary conditions at $y = 0$

$$\begin{aligned} \sigma_y(x, 0, t) &= -\sigma_1 q_1(x) f(t), & \text{for } |x| < a \\ \tau_{xy}(x, 0, t) &= 0, & \text{for } 0 < |x| < \infty \\ v(x, 0, t) &= 0, & \text{for } |x| > a. \end{aligned} \quad (4)$$

In addition the condition on displacement at infinity is

$$\lim_{x^2 + y^2 \rightarrow \infty} [u(x, y, t), v(x, y, t)] = 0.$$

The parameter σ_1 is a constant with the dimension of stress and $q_1(x)$ is restricted to functions that are even in x ; that is,

$$q_1(x) = q_1(-x).$$

Problem B—skew-symmetric in-plane shear

In this case in-plane tangential tractions only are suddenly applied to the crack surface. The initial conditions are again zero and the boundary conditions are :

$$\begin{aligned} \sigma_y(x, 0, t) &= 0, & \text{for } 0 < |x| < \infty \\ \tau_{xy}(x, 0, t) &= -\sigma_2 q_2(x) f(t), & \text{for } |x| < a \\ u(x, 0, t) &= 0, & \text{for } |x| > a \end{aligned} \tag{5}$$

and,

$$\lim_{x^2 + y^2 \rightarrow \infty} [u(x, y, t), v(x, y, t)] = 0$$

where σ_2 is a constant with the dimension of stress and where $q_2(x)$ is restricted to functions that are even in x . That is,

$$q_2(x) = q_2(-x).$$

DUAL INTEGRAL EQUATIONS

Recalling that the initial conditions are zero, the Laplace transform may be applied to equations (2) with the result

$$\nabla^2 \phi^* = (p/c_1)^2 \phi^*, \quad \nabla^2 \psi^* = (p/c_2)^2 \psi^* \tag{6}$$

with the Laplace transform pair being defined by the equations :

$$f^*(p) = \int_0^\infty f(t) \exp(-pt) dt, \quad f(t) = \frac{1}{2\pi i} \int_{Br} f^*(p) \exp(pt) dp$$

where the second integral is over the Bromwich path [14].

In order to reduce equations (6) to ordinary differential equations the Fourier cosine and sine transforms will be applied. The Fourier cosine transform pair is

$$\hat{f}(\alpha) = \int_0^\infty f(x) \cos(\alpha x) dx, \quad f(x) = \frac{2}{\pi} \int_0^\infty \hat{f}(\alpha) \cos(\alpha x) d\alpha$$

and the Fourier sine transform pair is

$$\hat{f}(\alpha) = \int_0^\infty f(x) \sin(\alpha x) dx, \quad f(x) = \frac{2}{\pi} \int_0^\infty \hat{f}(\alpha) \sin(\alpha x) d\alpha.$$

The application of these transforms will depend on whether the function under consideration is even or odd in x and will be considered separately for problems A and B.

Problem A

By consideration of the symmetry properties of the boundary conditions it can be shown that for this case,

$$\phi(x, y, t) = \phi(-x, y, t), \quad \psi(x, y, t) = -\psi(-x, y, t)$$

and the solution may be considered in the first quadrant of the plane.

Then, the Fourier cosine transform is applied to the function ϕ^* and the Fourier sine transform is applied to ψ^* in equations (6), the result being,

$$\begin{aligned}\frac{d^2\bar{\phi}^*}{dy^2} - [\alpha^2 + (p/c_1)^2]\bar{\phi}^* &= 0 \\ \frac{d^2\hat{\psi}^*}{dy^2} - [\alpha^2 + (p/c_2)^2]\hat{\psi}^* &= 0.\end{aligned}\quad (7)$$

Solutions to equations (7) that satisfy the regularity conditions at infinity are

$$\begin{aligned}\bar{\phi}^* &= \frac{\pi}{2}A_1(\alpha, p) \exp(-\gamma_1 y) \\ \hat{\psi}^* &= \frac{\pi}{2}B_1(\alpha, p) \exp(-\gamma_2 y)\end{aligned}\quad (8)$$

provided that the α -plane is cut so that,

$$\sqrt{[\alpha^2 + (p/c_j)^2]} \geq 0, \quad -\infty < \alpha < \infty \quad (j = 1, 2).$$

The inverse Fourier transforms of equations (8) are

$$\begin{aligned}\phi^* &= \int_0^\infty A_1(\alpha, p) \exp(-\gamma_1 y) \cos(\alpha x) \, d\alpha \\ \psi^* &= \int_0^\infty B_1(\alpha, p) \exp(-\gamma_2 y) \sin(\alpha x) \, d\alpha.\end{aligned}\quad (9)$$

The quantities γ_1 and γ_2 in equations (8) and (9) are defined as

$$\gamma_1 = \sqrt{[\alpha^2 + (p/c_1)^2]}, \quad \gamma_2 = \sqrt{[\alpha^2 + (p/c_2)^2]}.$$

By combining the Laplace transform of τ_{xy} with ϕ^* and ψ^* , the second boundary condition in equations (4) may be expressed in the form,

$$\int_0^\infty \{\alpha\gamma_1 A_1(\alpha, p) - [\alpha^2 + \frac{1}{2}(p/c_2)^2]B_1(\alpha, p)\} \sin(\alpha x) \, d\alpha = 0, \quad 0 < x < \infty.$$

The preceding equation is satisfied for all x by defining a new function $D_1(\alpha, p)$ such that

$$A_1(\alpha, p) = \frac{[\alpha^2 + \frac{1}{2}(p/c_2)^2]}{\gamma_1} D_1(\alpha, p), \quad B_1(\alpha, p) = \alpha D_1(\alpha, p).$$

Then, referring to equations (9), ϕ^* and ψ^* may be written as

$$\begin{aligned}\phi^* &= \int_0^\infty \frac{1}{\gamma_1} \left(1 + \frac{1}{2\alpha^2 k^2}\right) D_1(\alpha, p) \exp(-\gamma_1 y) \cos(\alpha x) \alpha^2 \, d\alpha \\ \psi^* &= \int_0^\infty D_1(\alpha, p) \exp(-\gamma_2 y) \sin(\alpha x) \alpha \, d\alpha\end{aligned}\quad (10)$$

with the parameter k defined as,

$$k = c_2/p.$$

Finally the first and third boundary conditions in equations (4) may be applied by substituting equations (10) into the Laplace transforms of σ_y and v . The resulting set of dual integral equations is

$$\int_0^\infty g_1(\alpha k) D_1(\alpha, p) \cos(\alpha x) \alpha \, d\alpha = \frac{\sigma_1 q_1(x) f^*(p)}{\rho p^2}, \quad |x| < a$$

$$\int_0^\infty D_1(\alpha, p) \cos(\alpha x) \, d\alpha = 0, \quad |x| > a$$
(11)

where $f^*(p)$ is the Laplace transform of the function $f(t)$ in the first of equations (4) and where

$$g_1(k) = 2k^2 [1 + (c_0/k)^2]^{-\frac{1}{2}} \left\{ \left(1 + \frac{1}{2k^2} \right)^2 - \left(1 + \frac{1}{k^2} \right)^{\frac{1}{2}} [1 + (c_0/k)^2]^{\frac{1}{2}} \right\}$$

with

$$c_0 = c_2/c_1.$$

Problem B

In this case consideration of symmetry in the boundary conditions leads to the following properties of ϕ and ψ .

$$\phi(x, y, t) = -\phi(-x, y, t), \quad \psi(x, y, t) = \psi(-x, y, t).$$

Then, by similar reasoning to that used for problem A, integral representations of the Laplace transforms of ϕ and ψ may be written in the form

$$\phi^* = \int_0^\infty D_2(\alpha, p) \exp(-\gamma_1 y) \sin(\alpha x) \alpha \, d\alpha$$

$$\psi^* = - \int_0^\infty \frac{1}{\gamma_2} \left(1 + \frac{1}{2\alpha^2 k^2} \right) D_2(\alpha, p) \exp(-\gamma_2 y) \cos(\alpha x) \alpha^2 \, d\alpha.$$
(12)

These expressions automatically satisfy the first of equations (5) while the remaining boundary conditions require that $D_2(\alpha, p)$ be the solution to the following set of dual integral equations

$$\int_0^\infty g_2(\alpha k) D_2(\alpha, p) \cos(\alpha x) \alpha \, d\alpha = \frac{\sigma_2 q_2(x) f^*(p)}{\rho p^2}, \quad |x| < a$$

$$\int_0^\infty D_2(\alpha, p) \cos(\alpha x) \, d\alpha = 0, \quad |x| > a$$
(13)

with

$$g_2(k) = 2k^2 \left(1 + \frac{1}{k^2} \right)^{-\frac{1}{2}} \left\{ \left(1 + \frac{1}{2k^2} \right)^2 - \left(1 + \frac{1}{k^2} \right)^{\frac{1}{2}} [1 + (c_0/k)^2]^{\frac{1}{2}} \right\}.$$

SOLUTION OF DUAL INTEGRAL EQUATIONS

The form of the dual integral equations is the same for both problems *A* and *B*. In order to put these equations in a form amenable to solution, the first equation in each set of the dual integral equations is integrated with respect to x over the interval $(0, x)$. The result for both problems may be summarized as follows:

$$\int_0^\infty g_j(\alpha k) D_j(\alpha, p) \sin(\alpha x) d\alpha = \frac{\sigma_j Q_j(x) f^*(p)}{\rho p^2}, \quad |x| < a$$

$$\int_0^\infty D_j(\alpha, p) \cos(\alpha x) d\alpha = 0, \quad |x| > a$$
(14)

where $j = 1, 2$ and

$$Q_j(x) = \int_0^x q_j(s) ds.$$

The subscript j is equal to 1 for problem *A* and 2 for problem *B*.

Following the usual argument [15] for solution of dual integral equations, a displacement related function $h_j^*(x, p)$ is defined by the equation,

$$h_j^*(x, p) = \frac{2}{\pi} \int_0^\infty D_j(\alpha, p) \cos(\alpha x) d\alpha$$
(15)

where $h_j^*(x, p)$ must be zero for $|x| > a$ as required by equation (14). Hence the Fourier inversion theorem leads to the expression,

$$D_j(\alpha, p) = \int_0^a h_j^*(x, p) \cos(\alpha x) dx.$$
(16)

The function $h_j^*(x, p)$ is to be constructed to possess the proper asymptotic behavior at the crack border so that the near-field displacement is proportional to the square root of the distance from the crack edge. To this end, let

$$h_j^*(x, p) = \int_x^a \frac{U_j^*(\tau, p) \tau d\tau}{\sqrt{(\tau^2 - x^2)}}, \quad |x| < a.$$
(17)

Substitution of equation (17) into (16) and application of the identity

$$\int_0^\tau \frac{\cos(\alpha x) dx}{\sqrt{(\tau^2 - x^2)}} = \frac{\pi}{2} J_0(\alpha \tau)$$
(18)

where J_0 denotes the zero-order Bessel function of the first kind, leads to the expression

$$D_j(\alpha, p) = \frac{\pi}{2} \int_0^a U_j^*(\tau, p) J_0(\alpha \tau) \tau d\tau.$$
(19)

In order to rewrite the first of equations (14) as an Abel's integral equation for $U_j^*(\tau, p)$ a function $w_j(\alpha k)$ is introduced such that

$$w_j(\alpha k) = (1 - c_0^2) - g_j(\alpha k).$$
(20)

By virtue of equations (19) and (20), the governing integral equation takes the form

$$(1 - c_0^2) \int_0^a \left[U_j^*(\tau, p) \tau \int_0^\infty J_0(\alpha\tau) \sin(\alpha x) \, d\alpha \right] d\tau = \frac{2}{\pi} \frac{\sigma_j Q_j(x) f^*(p)}{\rho p^2} + \int_0^a \left[U_j^*(\tau, p) \tau \int_0^\infty w_j(\alpha k) J_0(\alpha\tau) \sin(\alpha x) \, d\alpha \right] d\tau. \tag{21}$$

Using the identity

$$\int_0^\infty J_0(\alpha\tau) \sin(\alpha x) \, d\alpha = \begin{cases} 0, & 0 < x < \tau \\ (x^2 - \tau^2)^{-\frac{1}{2}}, & x > \tau \end{cases}$$

the desired form of Abel's integral equation is obtained

$$(1 - c_0^2) \int_0^x \frac{U_j^*(\tau, p) \tau \, d\tau}{\sqrt{(x^2 - \tau^2)}} = \frac{2}{\pi} \frac{\sigma_j Q_j(x) f^*(p)}{\rho p^2} + \int_0^a \left[U_j^*(\tau, p) \tau \int_0^\infty w_j(\alpha k) J_0(\alpha\tau) \sin(\alpha x) \, d\alpha \right] d\tau, \quad |x| < a.$$

Inversion of the preceding equation yields

$$(1 - c_0^2) U_j^*(\tau, p) = \frac{2}{\pi} \int_0^\tau \frac{1}{\sqrt{(\tau^2 - x^2)}} \left\{ \frac{2}{\pi} \frac{\sigma_j Q_j(x) f^*(p)}{\rho p^2} + \int_0^a \left[U_j^*(\zeta, p) \zeta \int_0^\infty w_j(\alpha k) J_0(\alpha\zeta) \cos(\alpha x) \alpha \, d\alpha \right] d\zeta \right\} dx, \quad \tau < a. \tag{22}$$

Now, introduce the non-dimensional variables

$$\xi = \tau/a, \quad \eta = \zeta/a, \quad s = \alpha a, \quad z = x/a$$

and define

$$\begin{aligned} \kappa &= k/a, & \beta_j(z) &= w_j(za) \\ \Lambda_j^*(\xi, \kappa) &= \frac{\pi}{2} (1 - c_0^2) \frac{\rho p^2 \sqrt{(\xi)} U_j^*(\xi a, p)}{\sigma_j f^*(p)}. \end{aligned}$$

Then, making use of equation (18), equation (22) may be written in the form of a standard Fredholm integral equation of the second kind

$$\Lambda_j^*(\xi, \kappa) - \int_0^1 \Lambda_j^*(\eta, \kappa) K_j(\xi, \eta) \, d\eta = \frac{2}{\pi} \sqrt{\xi} \int_0^\xi \frac{\beta_j(z) \, dz}{\sqrt{(\xi^2 - z^2)}} \tag{23}$$

whose kernel, being symmetric in ξ and η , is

$$K_j(\xi, \eta) = \frac{\sqrt{(\xi\eta)}}{(1 - c_0^2)} \int_0^\infty s w_j(s\kappa) J_0(s\eta) J_0(s\xi) \, ds, \quad 0 < \xi \leq 1; \quad 0 < \eta \leq 1.$$

For rapid convergence of the infinite integral, define a function $d_j(\kappa)$ as

$$d_j(\kappa) = w_j(\kappa) + \frac{H_j}{\kappa^2 + E_j^2}, \quad j = 1, 2$$

where, in order that $d_j(\kappa)$ be of order $(\kappa)^{-6}$ for large κ , H_j and E_j^2 are chosen as

$$H_1 = \frac{1}{4}(3c_0^4 - 4c_0^2 + 3)$$

$$H_2 = \frac{1}{4}(1 + c_0^4)$$

$$E_1^2 = \frac{1}{8H_1}(5c_0^6 - 6c_0^4 + 2c_0^2 + 1)$$

$$E_2^2 = \frac{1}{8H_2}(1 + c_0^6).$$

Since

$$\int_0^\infty \frac{H_j}{(s\kappa)^2 + E_j^2} J_0(s\eta) J_0(s\xi) s ds = \frac{H_j}{\kappa^2} I_0\left(\frac{E_j \xi}{\kappa}\right) K_0\left(\frac{E_j \eta}{\kappa}\right), \quad 0 < \xi \leq \eta$$

the expression for the kernel in the Fredholm integral equation becomes

$$K_f(\xi, \eta) = \frac{\sqrt{(\xi\eta)}}{1 - c_0^2} \left[-\frac{H_j}{\kappa^2} I_0\left(\frac{\xi E_j}{\kappa}\right) K_0\left(\frac{\eta E_j}{\kappa}\right) + \int_0^\infty s d_j(s\kappa) J_0(s\eta) J_0(s\xi) ds \right], \quad 0 < \xi \leq \eta$$

where I_0 and K_0 are the zero-order modified Bessel's functions of the first and second kind, respectively.

Making use of equation (19) and the definition of Λ_j^* the unknown function $D_j(\alpha, p)$ may be written in terms of the solution of the Fredholm integral equation as,

$$D_f(\alpha, p) = \frac{\sigma_f a^2 f^*(p)}{(1 - c_0^2) \rho p^2} \int_0^1 \left[\frac{\Lambda_j^*(\xi, \kappa)}{\sqrt{\xi}} \right] J_0(\alpha a \xi) \xi d\xi.$$

This expression may be integrated by parts with the result

$$D_f(\alpha, p) = \frac{\sigma_f a f^*(p)}{(1 - c_0^2) \rho p^2 \alpha} \left\{ \Lambda_j^*(1, \kappa) J_1(\alpha a) - \int_0^1 \frac{d}{d\xi} \left[\frac{\Lambda_j^*(\xi, \kappa)}{\sqrt{\xi}} \right] J_1(\alpha a \xi) \xi d\xi \right\} \quad (24)$$

from which the stresses and displacements may be determined.

TIME DEPENDENT STRESS FIELD

The integral expressions for the Laplace transforms of the potentials ϕ and ψ are now completely determined and, making use of equations (3), corresponding expressions for the Laplace transforms of the dynamic stresses may be obtained. It remains then to take the inverse Laplace transforms. This may be accomplished by applying the Cagniard DeHoop inversion technique [16, 17]. Due to the complexity of calculation, the detailed procedure will be given only for the first stress invariant $\sigma_x + \sigma_y$. From equations (3) and (6) the Laplace transform of $\sigma_x + \sigma_y$ is

$$\sigma_x^* + \sigma_y^* = -2\rho p^2 (1 - c_0^2) \phi_j^*, \quad j = 1, 2 \quad (25)$$

where the j subscript has been added to distinguish between the problem with normal tractions and the problem with shear tractions.

The part of the solution of interest here is the singular solution near the crack tip. For this portion of the solution it is easily shown [15] that only the first term on the right hand

side of equation (24) need be retained. The integral expression in $D_f(\alpha, p)$ is associated with terms that remain finite at the crack tip.

Problem A—(j = 1)

Putting ϕ^* in equations (10) into (25), the near-field solution for $\sigma_x + \sigma_y$ in the transformed plane is

$$\sigma_x^* + \sigma_y^* = -2\sigma_1 a f^*(p) \Lambda_1^*(1, \kappa) \int_0^\infty \frac{1}{\alpha \gamma_1} [\alpha^2 + \frac{1}{2}(p/c_2)^2] J_1(\alpha a) \exp(\gamma_1 y) \cos(\alpha x) d\alpha.$$

Changing the variable of integration to $\alpha = wp$ and noting that $J_1(apw)$ is an odd function with respect to w , the above becomes

$$\sigma_x^* + \sigma_y^* = -\sigma_1 a f^*(p) \Lambda_1^*(1, \kappa) p \int_{-\infty}^\infty T(w) J_1(apw) \exp[-p(\sqrt{(w^2 + c_1^{-2})}y - iwX)] dw \quad (26)$$

in which $T(w)$ stands for

$$T(w) = \frac{w^2 + (1/2c_2^2)}{w\sqrt{[w^2 + (1/c_1^2)]}}.$$

Making use of the identity [18],

$$J_1(x) = \frac{i}{\pi} \int_0^\pi \exp(-ix \cos \omega) \cos \omega d\omega$$

equation (26) further simplifies to

$$\begin{aligned} \sigma_x^* + \sigma_y^* = & -\frac{ia\sigma_1 p}{\pi} f^*(p) \Lambda_1^*(1, \kappa) \int_0^\pi \cos \omega \\ & \times d\omega \left\{ \int_{-\infty}^\infty T(w) \exp[-p(\sqrt{(w^2 + c_1^{-2})}y - iwX)] dw \right\}. \end{aligned} \quad (27)$$

The variable X is given by

$$X = x - a \cos \omega.$$

To evaluate equation (27), consider first the function I_1^* defined by the relation

$$I_1^* = \int_0^\pi \cos \omega d\omega \int_0^\infty T(w) \exp[-p(\sqrt{(w^2 + c_1^{-2})}y - iwX)] dw. \quad (28)$$

This function is in a form suitable for evaluation through the Cagniard-DeHoop method. The objective here is to transform the integral on the right side of equation (28) into a recognizable Laplace transform. This may be done by making the change in variables,

$$\tau = \sqrt{(w^2 + c_1^{-2})}y - iwX.$$

Solving for w as a function of τ gives

$$w = \pm \sqrt{[\tau^2 - (R/c_1)^2]} \frac{y}{R^2} + \frac{iX\tau}{R^2} \quad (29)$$

in which $R^2 = X^2 + y^2$ and $y = X \tan \beta$ where β is defined in Fig. 2.

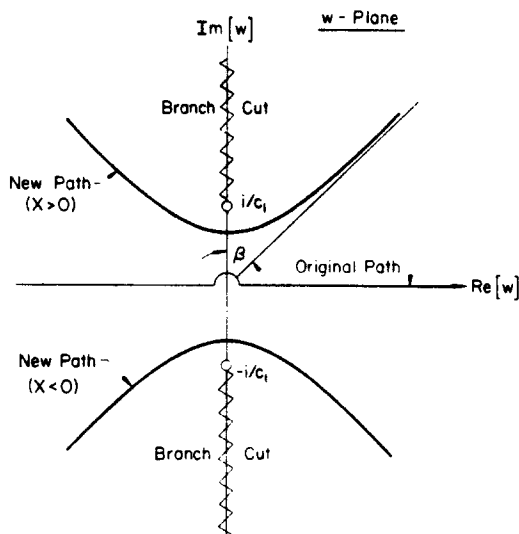


FIG. 2. Path of integration in w -plane.

The remainder of the procedure consists of treating w as a complex variable and locating a path in the w -plane along which τ is a positive number. Referring to Fig. 2 and noting that the integrand in equation (28) possesses branch points at $\pm ic_1$, cuts are made in the w -plane as shown in order that the function $(w^2 + 1/c_1^2)^{\frac{1}{2}}$ be single valued and have a real part that is positive everywhere in the w -plane. If τ is restricted to real non-negative values, equation (29) is the equation of a hyperbola in the w -plane. If $X > 0$ ($X < 0$) the hyperbola will be in the upper (lower) half of the w -plane. The path of integration in equation (28) can be converted from the real axis to the aforementioned hyperbola by making use of the Cauchy integral theorem and Jordan's lemma. Thus, after changing the variable of integration to τ by means of equation (29), it is found that

$$I_1^* = \int_0^\pi \cos \omega \, d\omega \int_{R/c_1}^\infty \left[T(w^+) \frac{dw^+}{d\tau} - T(w^-) \frac{dw^-}{d\tau} \right] \exp(-p\tau) \, d\tau \tag{30}$$

where the (+) and (-) superscripts refer to the right (left) hand legs of the hyperbola. Noting that the inner integral is in the form of a Laplace transform it is a matter of inspection to write the inverse Laplace transform of I_1^* as

$$I_1(t) = \int_0^\pi H\left(t - \frac{R}{c_1}\right) \left[T(w^+) \frac{dw^+}{dt} - T(w^-) \frac{dw^-}{dt} \right] \cos \omega \, d\omega \tag{31}$$

where $H(t)$ is the Heaviside step function. Referring to equations (27) and (28) and making use of the convolution theorem for the Laplace transform, the stress invariant is obtained:

$$\sigma_x + \sigma_y = -\frac{ia\sigma_1}{\pi} \int_0^t m_1(t - \tau) I_1(\tau) \, d\tau \tag{32}$$

where

$$m_1(t) = \mathcal{L}^{-1}[pf^*(p)\Lambda_1^*(1, \kappa)]$$

with \mathcal{L}^{-1} being the inverse Laplace transform operator.

In order to determine $\sigma_x + \sigma_y$ in the region near the crack tip it is necessary to extract the singular portion of $I_1(t)$ from equation (31). Without going into the mathematical details, it is easy to show that, as long as c_2t is sufficiently greater than r , the radial distance measured from the crack tip, I_1 is independent of time, i.e.

$$I_1 = -\frac{i}{a} \left[\int_{-a}^a \frac{q \, dq}{(q-z)\sqrt{(a^2-q^2)}} + \int_{-a}^a \frac{q \, dq}{(q-\bar{z})\sqrt{(a^2-q^2)}} \right]$$

with

$$z = x + iy, \quad \bar{z} = x - iy$$

and where the transformation of variables

$$q = a \cos \omega$$

has been made.

Making use of chapter 4 of Muskhelishvili [19] the evaluation of the above integrals near the crack tip leads to the following expression for the singular portion of I_1 ,

$$I_1 = \frac{2\pi i}{\sqrt{(2ar)}} \cos(\theta/2) + \dots$$

where r and θ are polar coordinates with the origin attached to the crack tip as shown in Fig. 1.

Then, referring to equation (32) it follows that the near field solution for the stress invariant is

$$\sigma_x + \sigma_y = \frac{2\sigma_1\sqrt{a}}{\sqrt{(2r)}} M_1(t) \cos(\theta/2) + \dots \tag{33}$$

where

$$M_1(t) = \int_0^t m_1(t) \, dt.$$

In a manner analogous to the static theory of brittle fracture, a dynamic stress intensity factor, $k_1(t)$ may be defined [20]:

$$k_1(t) = M_1(t)\sigma_1\sqrt{a}. \tag{34}$$

With this definition, the individual stress components may be evaluated, the result being

$$\begin{aligned} \sigma_x &= \frac{k_1(t)}{\sqrt{(2r)}} \cos(\theta/2) [1 - \sin(\theta/2) \sin(3\theta/2)] + \dots \\ \sigma_y &= \frac{k_1(t)}{\sqrt{(2r)}} \cos(\theta/2) [1 + \sin(\theta/2) \sin(3\theta/2)] + \dots \\ \tau_{xy} &= \frac{k_1(t)}{\sqrt{(2r)}} \cos(\theta/2) \sin(\theta/2) \cos(3\theta/2) + \dots \end{aligned} \tag{35}$$

Problem B—(j = 2)

The procedure here is the same as that for problem A. Following the operations performed in obtaining equations (27) the stress invariant for the skew-symmetric case is given by

$$\sigma_x^* + \sigma_y^* = -\frac{1}{\pi} a \sigma_1 p f^*(p) \Lambda_2^*(1, \kappa) \int_0^\pi \cos \omega \, d\omega \left\{ \int_{-\infty}^{\infty} \exp[-p(\sqrt{(w^2 + c_1^{-2})}y - iwX)] \, dw \right\}. \quad (36)$$

With the variable transformation of equation (29) the inversion procedure leads to the result,

$$\sigma_x + \sigma_y = -\frac{a\sigma_2}{\pi} \int_0^t m_2(t-\tau) I_2(\tau) \, d\tau \quad (37)$$

where

$$I_2(t) = \int_0^\pi H\left(t - \frac{R}{c_1}\right) \left[\frac{dw^+}{dt} - \frac{dw^-}{dt} \right] \cos \omega \, d\omega$$

and

$$m_2(t) = \mathcal{L}^{-1}[pf^*(p)\Lambda_2^*(1, \kappa)].$$

As in the symmetric case the singular portion of the solution may be isolated in the neighborhood of the crack tip with the result that

$$\sigma_x + \sigma_y = -\frac{2\sigma_2\sqrt{a}}{\sqrt{2r}} M_2(t) \sin(\theta/2) + \dots \quad (38)$$

in which

$$M_2(t) = \int_0^t m_2(t) \, dt.$$

Again a dynamic stress-intensity factor $k_2(t)$ may be defined

$$k_2(t) = M_2(t) \sigma_2 \sqrt{a} \quad (39)$$

and the individual stress components, in the neighborhood of the crack tip become

$$\begin{aligned} \sigma_x &= -\frac{k_2(t)}{\sqrt{(2r)}} \sin(\theta/2) [2 + \cos(\theta/2) \cos(3\theta/2)] + \dots \\ \sigma_y &= \frac{k_2(t)}{\sqrt{(2r)}} \sin(\theta/2) \cos(\theta/2) \cos(3\theta/2) + \dots \\ \tau_{xy} &= \frac{k_2(t)}{\sqrt{(2r)}} \cos(\theta/2) [1 - \sin(\theta/2) \sin(3\theta/2)] + \dots \end{aligned} \quad (40)$$

This completes the analysis for the dynamic crack-tip stress field which is an essential piece of information in the application of the current theory of fracture mechanics. The amount of energy released by the crack during the impact loading as described in the boundary conditions of this problem can be related to $k_1(t)$ and $k_2(t)$. For details, refer to a paper by Sih [20].

CONCLUDING REMARKS

Through the analysis of the preceding sections, it has been shown that the stress field very near the crack tip has the same spatial distribution for the dynamic case as for the static case, the only difference being that the intensity of the field is a function of time. The time dependent stress-intensity factors $k_1(t)$ and $k_2(t)$, being related to the functions $m_1(t)$ and $m_2(t)$, depend ultimately on the functions $\Lambda_j^*(1, \kappa)$ for various values of the Laplace transform variable p . Inversion of the Laplace transform numerically then enables the evaluation of $m_j(t)$ and thus $k_j(t)$ for both problems $A(j = 1)$ and $B(j = 2)$. The procedure used for this is described in Ref. [3].

For both modes of loading considered here, numerical results have been obtained for the case of a uniform load σ_j suddenly applied to the crack surface. That is, $q_j(x)$ is a constant and $f(t)$ is the Heaviside step function $H(t)$. By superposition this type of loading corresponds to the sudden appearance of a crack in a stressed plate. The solutions of the Fredholm integral equations, $\Lambda_j^*(1, \kappa)$ ($j = 1, 2$), are plotted as a function of c_2/pa for both normal impact and shear impact in Fig. 4.

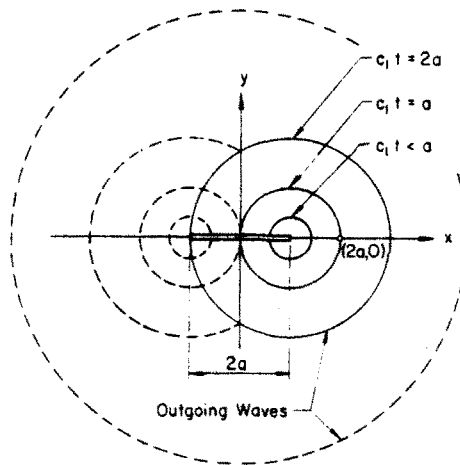


FIG. 3. Wave fronts emanating from crack tip.

In Fig. 5 the dynamic stress-intensity factors, k_j ($j = 1, 2$) normalized with respect to the corresponding static values are plotted as a function of $c_2 t/a$. The ratio of shear wave speed c_2 to dilatational speed c_1 that was used is 0.542, the value for steel. The results for mode III, or anti-plane strain loading, previously reported by Ravera and Sih [13], is also included for comparison. Although the stress-intensity factors for the three modes peak at different times and possess different maximum values, the character of the three solutions is the same. That is the stress-intensity factor reaches a peak greater than the static value and subsequently oscillates about the value with decreasing amplitude.

These results are in agreement with the experimental results of Soltesz and Sommer [11] mentioned earlier. Measurements of the crack opening displacement, which is directly related to the stress-intensity factor, showed that k_1 reached a maximum at approximately

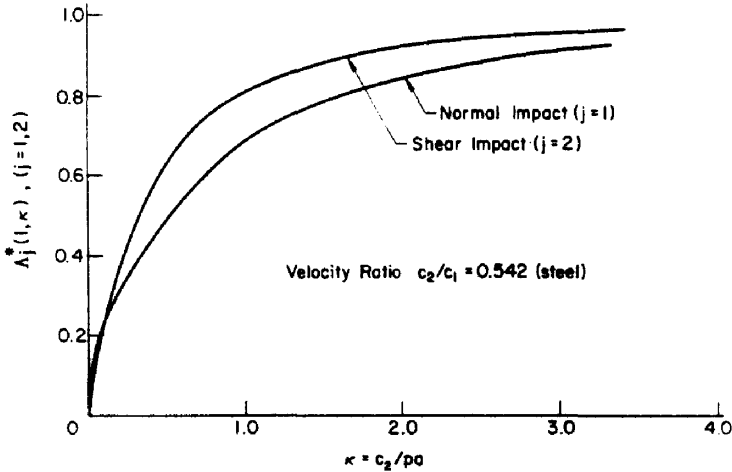


FIG. 4. Solution to the Fredholm integral equation.

10^{-5} sec, the same order of magnitude as obtained here. The oscillations that were observed in crack opening displacement were explained as due to a combination of wave reflection at the edges of the finite plate and oscillation in the k_1 value due to the initially applied load, i.e. the result demonstrated in this paper.

In order to gain further insight into the response of the cracked plate it is useful to review the wave pattern. When a transient load is applied to the crack surface, the results, aside from wave propagation from the loaded surface is that the crack tips form the center of two outgoing cylindrical waves. For the period of time, t_s , before these waves begin to

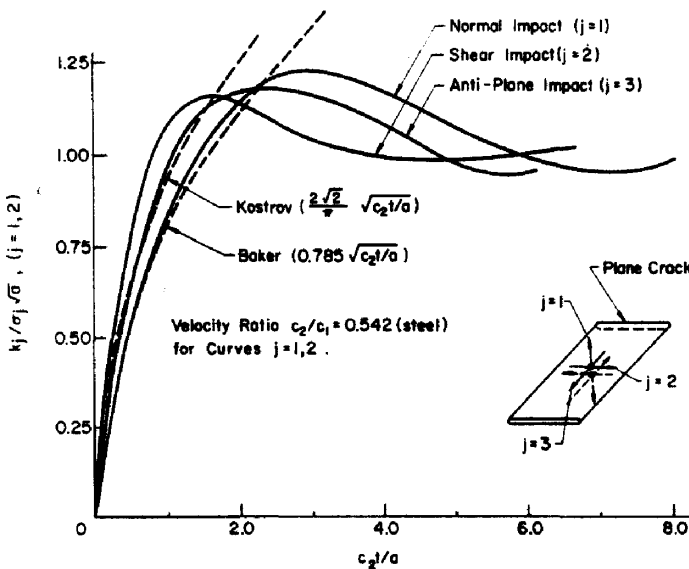


FIG. 5. Dynamic stress-intensity factors.

interact the short time behavior of the solution is described by the equations

$$\sigma_{ik} = \frac{k_j^{(s)}}{\sqrt{(2r)}} f_{ik}(\theta), \quad 0 < t < t_s \quad \text{and} \quad j = 1, 2 \quad (41)$$

where r is the distance from the crack tip, and

$$k_j^{(s)} \sim \sqrt{t}, \quad j = 1, 2.$$

The function $f_{ik}(\theta)$ is the same as in the static case. Since the disturbance at one crack tip is not yet affected by the presence of the other crack tip this is the range for which the solution to the problem of sudden loading on a semi-infinite crack is valid. For anti-plane strain and normal loading the stress-intensity factors may be obtained from the solutions of Kostrov [5] and Baker [10]. These are

$$k_1^{(s)} = 0.785\sqrt{(c_2t/a)}\sigma_1\sqrt{a} \quad (42)$$

for the case of steel in mode I loading and

$$k_3^{(s)} = \frac{2\sqrt{2}}{\pi}\sqrt{(c_2t/a)}\sigma_3\sqrt{a} \quad (43)$$

for mode III loading.

These results are plotted in Fig. 5 and show good agreement with the numerical solutions obtained here.

The stress wave pattern loses its geometrical simplicity after the two cylindrical waves begin to interact although, very close to the crack tip, the angular distribution and square root singularity remain the same. It is during this period of maximum disorder that the stress-intensity factor takes on a maximum value.

By allowing a sufficient time to elapse, say $c_2t \gg 2a$, the wave pattern merges into a single outgoing wave surrounding the entire crack. It was for the range that Ravera and Sih [13] explicitly extracted a near-field solution although it may be argued as in this paper that the near field solution thus obtained is actually valid over the much larger range of time. The method used here to determine the asymptotic behavior of the near field stress solution requires only that the stress-wave boundary be well beyond the region of interest. Thus, if the stress field is to be valid within a distance r of the crack tip, the condition on the time elapsed is $c_2t \gg r$. As long as r is kept small enough it may be said that the solution is valid for all time. The condition on r is of course in addition to the static restriction that $r \ll a$. This restriction was also discussed by Sih and Embley [3] for the case of torsional loading of a penny-shaped crack.

Recently, Thau and Lu [21] have found the dynamic stress-intensity factor for the case of a crack engulfed by an obliquely incident dilatational wave. They used the generalized Wiener-Hopf technique and found that the stress-intensity factor reached a peak in the time for the Rayleigh wave to travel from one crack tip to the other. At the peak there is a discontinuity in the slope of the stress-intensity factor curve which is smoothed out in the numerical calculations presented here. In general, the present results agree well with those in [21] and this gives an additional verification to the reliability of the numerical method employed in this paper.

REFERENCES

- [1] G. C. SIH, Some elastodynamic problems of cracks. *Int. J. Fracture Mech.* 4, 51–68 (1968).
- [2] G. T. EMBLEY and G. C. SIH, Response of a Penny Shaped Crack to Impact Waves, *Proceedings of the 12th Midwestern Mechanics Conference* (1971).
- [3] G. C. SIH and G. T. EMBLEY, Sudden twisting of a penny-shaped crack, to be published.
- [4] L. M. FLITMAN, Waves caused by a sudden crack in a continuous elastic medium. *PMM* 27, 938–953 (1963).
- [5] B. V. KOSTROV, Unsteady propagation of longitudinal shear cracks. *PMM* 30, 1241–1248 (1966).
- [6] J. D. ESHELBY, The elastic field of a crack extending non-uniformly under general anti-plane loading. *J. Mech. Phys. Solids* 17, 177–199 (1969).
- [7] J. D. ACHENBACH, Crack propagation generated by a horizontally polarized shear wave. *J. Mech. Phys. Solids* 18, 245–259 (1970).
- [8] J. D. ACHENBACH, Brittle and ductile extension of a finite crack by a horizontally polarized shear wave. *Int. J. Engng Sci.* 8, 947–966 (1970).
- [9] A. W. MAUE, Die Spannungswelle bei plötzlichem Einschnitt eines gespannten elastischen Körpers. *Z. angew. Math. Mech.* 34, 1–12 (1954).
- [10] B. R. BAKER, Dynamic stresses created by a moving crack. *J. appl. Mech.* 29, 449–454 (1962).
- [11] U. SOLTESZ and E. SOMMER, Crack-opening–displacement measurement of a dynamically loaded crack. *J. Engng Fracture Mech.* in press.
- [12] I. N. SNEDDON, *Fourier Transforms*. McGraw-Hill (1951).
- [13] R. J. RAVERA and G. C. SIH, Transient analysis of stress waves around cracks under antiplane strain. *J. acoust. Soc. Am.* 47, 875–881 (1970).
- [14] G. DOETSCH, *Guide to the Applications of Laplace Transforms*. Van Nostrand (1961).
- [15] G. C. SIH and J. F. LOEBER, Wave propagation in an elastic solid with a line of discontinuity or finite crack. *Q. appl. Math.* 27, 193 (1969).
- [16] L. CAGNIARD, *Reflection and Refraction of Progressive Seismic Waves*. McGraw-Hill (1962).
- [17] A. T. DEHOOP, A modification of Cagniard's method for solving seismic pulse problems. *Appl. Sci. Res.* 8, 344–356 (1960).
- [18] G. N. WATSON, *A Treatise on the Theory of Bessel Functions*. MacMillan (1948).
- [19] N. I. MUSKHELISHVILI, *Singular Integral Equations*. Noordhoff (1953).
- [20] G. C. SIH, Dynamic Aspects of Crack Propagation, in *Inelastic Behavior of Solids*, pp. 607–639, McGraw-Hill (1970).
- [21] S. A. THAU and T. H. LU, Transient stress intensity factors for a finite crack in an elastic solid caused by a dilatational wave. *Int. J. Solids Struct.* 7, 731–750 (1971).

(Received 27 July 1971)

Абстракт—Используя интегральные преобразования, сопряженные с методом Каниарда, определяются нестационарные напряжения и поля перемещений, вокруг конечной трещины, раскрытой нормальными и сдвиговыми силами расщепления, приложенными к их поверхностям. Эти усилия приложены внезапно к шели, что представляет случай ударной нагрузки. Путем вычета однородного напряженного состояния, настоящее решение применяется также к задаче внезапного появления трещины в предварительно напряженном теле. Результаты указывают на значительную разницу между полученными факторами интенсивности динамических напряжений, для этой задачи, и такими же результатами для статической нагрузки. В особенности, энергия освобожденная динамически нагруженной трещиной, связана с фактором интенсивности напряжений, изменяется в зависимости от времени и достигает максимума очень быстро, а далее колеблется вокруг статического значения. Полученная информация пригодна для определения распространения шели под влиянием удара.